

Analytic continuation in the sinh-Gordon model

Patrick Dorey and Brandon Morrison

Abstract We study the analytic continuation of the finite-volume energy levels of the sinh-Gordon model. The structure is surprisingly rich, and in the small-coupling limit we find systematic patterns which suggest that a complete picture may be possible.

1 Introduction

The idea that different states in a quantum theory might be linked by a process of analytic continuation in a parameter is an old one, perhaps most spectacularly realised in Bender and Wu's analysis of the quantum anharmonic oscillator [2]. It is natural to ask whether a similar level of understanding could be attained for a quantum field theory, and in this short note we describe some steps in this direction.

Our main focus will be the quantum sinh-Gordon model, an integrable quantum field theory in 1+1 dimensions. But to illustrate the main idea we start with a much simpler example, discussed in [6]: the finite volume spectrum of the 1+1 dimensional Ising field theory. With the spatial dimension curled up to form a circle of circumference R , the ground state energy can be written as [9]

$$E_0(M, R) = E_{\text{bulk}}(M, R) - \frac{\pi}{6R} c_0^{(\text{Ising})}(MR),$$

where M the inverse of the bulk correlation length, $E_{\text{bulk}}(M, R)$ contains the bulk contribution, and $c_0^{(\text{Ising})}(MR)$, the so-called effective central charge for the Ising

Patrick Dorey
Durham University, UK
e-mail: p.e.dorey@durham.ac.uk

Brandon Morrison
Durham University, UK
e-mail: brandon.m.morrison@dunelm.org.uk

field theory, is given in closed form by the following expression:

$$c_0^{(\text{Ising})}(r) = \frac{1}{2} - \frac{3r^2}{2\pi^2} \left(\log \frac{1}{r} + \frac{1}{2} + \ln \pi - \gamma_E \right) \\ + \frac{6}{\pi} \sum_{k=1}^{\infty} \left(\sqrt{r^2 + (2k-1)^2 \pi^2} - (2k-1)\pi - \frac{r^2}{2(2k-1)\pi} \right)$$

with $r = MR$ and $\gamma_E = 0.57721566\dots$. Apart from the logarithmic singularity at the origin, $c_0(r)$ has a sequence of square-root singularities in the complex r plane, at odd-integer multiples of $i\pi$. If R (or equivalently r) is continued along a closed path from the positive real axis, around the singularities with $k = k_1, k_2, \dots, k_n$ and back, then the corresponding square roots will flip signs from positive to negative, decreasing $c_0(r)$, and thereby increasing $E_0(R)$ to

$$E_{k_1, k_2, \dots, k_n}(M, R) = E_0(M, R) + \frac{2}{R} \sum_{i=1}^n \sqrt{r^2 + (2k_i-1)^2 \pi^2}$$

which is the energy of an excited state of the model, containing $2n$ Bethe-quantised particles in the infrared.

In more general, interacting cases, an explicit representation of the finite-volume ground state energy is not available, and so the analysis above cannot be applied directly. However, when the quantum field theory in question is integrable with a known exact S-matrix, $E_0(R)$ can be expressed in terms of solutions the relevant thermodynamic Bethe Ansatz (TBA) equations [11]. For a theory with a single scalar particle of mass M and exact scattering matrix $S(\theta)$ (where θ is the rapidity), confined to live on a circle of circumference R , the recipe is as follows. First, find the so-called pseudoenergy $\varepsilon(\theta)$ by solving the following non-linear integral equation (the TBA equation)

$$\varepsilon(\theta) = r \cosh \theta - \phi * L(\theta),$$

where $r = MR$ is the system size in units of the correlation length, and

$$L(\theta) = \log \left(1 + e^{-\varepsilon(\theta)} \right), \\ f * g(\theta) = \frac{1}{2\pi} \int_{\mathbb{R}} f(\theta - \theta') g(\theta') d\theta', \\ \phi(\theta) = -i \frac{\partial}{\partial \theta} \log S(\theta).$$

Next, evaluate the effective central charge, also sometimes called a scaling function:

$$c_0(r) = \frac{3}{\pi^2} \int_{\mathbb{R}} r \cosh \theta L(\theta) d\theta.$$

In terms of this scaling function we have

$$E_0(R) = E_{\text{bulk}}(M, R) - \frac{\pi}{6R} c_0(r).$$

(Here $E_{\text{bulk}}(M, R)$ is a possible bulk term which will not play a role in the continuations we discuss below.) For the Ising case, $S(\theta) = -1$, so $\phi(\theta) = 0$ and the TBA equation is easily solved to yield the following alternative formula for $c_0^{(\text{Ising})}(r)$:

$$c_0^{(\text{Ising})}(r) = \frac{3}{\pi^2} \int_{\mathbb{R}} r \cosh \theta \log \left(1 + e^{-r \cosh \theta} \right) d\theta.$$

In the more interesting cases of interacting quantum field theories, $\phi(\theta)$ will be nontrivial and it won't be possible to solve for $\varepsilon(\theta)$ explicitly. Nevertheless, it is possible to track how the TBA equation itself changes under analytic continuation. This was studied in detail in [6], taking the Yang-Lee model (a perturbation of the $\mathcal{M}_{2,5}$ minimal model) as the initial example. The key is to keep track of the zeros of $1 + e^{-\varepsilon(\theta)}$, the argument of the logarithm in the definition of $L(\theta)$, in the complex θ plane. (By a small abuse of language we will sometimes refer to such points as singularities of the pseudoenergies, even though they are really only singularities of the associated functions $L(\theta)$.) For general r these will all be clear of the real axis. But if a pair of these zeros, say at θ_0 and $-\theta_0$, approach the real axis as r varies along some path¹, the TBA convolution risks becoming ill-defined. The solution is to distort the contour away from the real axis and around the singularities to allow them to cross over, which yields the correct analytic continuation of the equation. Returning the contour to the real axis generates a pair of residue terms, one each for the singularities at θ_0 and $-\theta_0$, which can be found explicitly via an integration by parts, as explained in [6]. The net result is that the TBA equation becomes

$$\varepsilon(\theta) = r \cosh \theta + \log \frac{S(\theta - \theta_0)}{S(\theta + \theta_0)} - \phi * L(\theta).$$

Likewise, the expression for $c_0(r)$ acquires an extra term, becoming

$$c(r) = \frac{12r}{\pi} i \sinh \theta_0 + \frac{3}{\pi^2} \int_{\mathbb{R}} r \cosh \theta L(\theta) d\theta.$$

This is no longer the effective central charge, but rather a scaling function associated with an excited state of the model. The new excited-state TBA equation might appear to have an extra unknown, θ_0 , the location of the singularity which has crossed the integration contour. This is fixed by the self-consistency requirement that $1 + e^{\varepsilon(\theta_0)} = 0$, or equivalently $\varepsilon(\theta_0) = (2N + 1)\pi i$ with $N \in \mathbb{Z}$.

In principle, this process can now be repeated, varying r again in the complex plane and looking for occasions when θ -plane singularities for the excited-state TBA equation cross the real axis, which will generate more complicated TBA equations corresponding to further excited states. At each stage the TBA equations found are exact, and some of their asymptotics can be evaluated exactly in small and large

¹ Since the TBA equation is symmetric in θ , the zeros in question are always paired in this way.

r limits. However, the ‘connectivity’ of these equations depends on how, and in what order, singularities of the pseudoenergies cross the TBA integration contour. This relies on the behaviour of solutions of the TBA equations at finite (and indeed complex) values of r , something which needs to be found numerically. In [6] (for the Yang-Lee model) and then [7] (for a further series of perturbed minimal models), the first few sheets of the Riemann surface of energy levels and the structure of the branch points linking them were found. However, and in spite of some further work with Lorenz Hilfiker and István Szécsényi [5], a complete picture for these theories has proved elusive: the arrangements of the low-lying levels do not show any clear patterns, and gathering more extensive data is made difficult by the fact that, even with the addition of damping factors, the numerical iteration of the TBA equations tends not to converge near branch points.

Instead, in the following we will report on some work on a different theory with more structure in the form of a tunable coupling, which will allow us to see evidence of a more uniform behaviour in the limit where this coupling is small: the sinh-Gordon model.

2 The sinh-Gordon model and its TBA equation

The infrared description of the sinh-Gordon model as a scattering theory is particularly simple: it is a theory of a single massive scalar particle, with an exact scattering matrix $S(\theta)$ which depends on a real parameter p lying between 0 and 1:

$$S(\theta) = \frac{\sinh(\theta) - i \sin(\pi p)}{\sinh(\theta) + i \sin(\pi p)}$$

This has physical strip zeros at $i\pi p$ and $i\pi(1-p)$. In the conventions of [13], p is related to the coupling b in the Euclidean action

$$A_{\text{ShG}} = \int \left[\frac{1}{4\pi} (\partial_\mu \phi)^2 + 2\mu \cosh 2b\phi \right] d^2x$$

by

$$p = \frac{b^2}{1+b^2}.$$

The strong-weak coupling duality of the model under $b \rightarrow 1/b$ is reflected in the symmetry of $S(\theta)$ under $p \rightarrow 1-p$, allowing p to be restricted to $0 < p \leq 1/2$.

The TBA equation for this model assumes the standard form given in the last section:

$$\varepsilon(\theta) = r \cosh \theta - \phi * L(\theta).$$

Since $S(\theta)$ has zeros at $\theta = i\pi p$ and $\theta = i\pi(1-p)$, and simple poles at $\theta = -i\pi p$ and $\theta = -i\pi(1-p)$, $\phi(\theta) = -i \frac{\partial}{\partial \theta} \log S(\theta)$ has simple poles at these same locations. Once the pseudoenergy has been found on the real axis, for example by numerical

iteration of the TBA equation, allowing θ to become complex provides a representation for the same function in the complex plane. However, due to the poles in the kernel $\phi(\theta)$, this only holds on the strip $-\pi p < \text{Im } \theta < \pi p$. To extend further, we can follow Aliosha Zamolodchikov [13] and define an associated pair of functions, $Y(\theta)$

$$Y(\theta) = e^{-\varepsilon(\theta)} = \exp\left(-r \cosh(\theta) + \frac{1}{2\pi} \int_{\mathbb{R}} \phi(\theta - \theta') L(\theta') d\theta'\right)$$

and $X(\theta)$

$$X(\theta) = \exp\left(-\frac{r}{2 \sin(\pi p)} \cosh(\theta) + \frac{1}{2\pi} \int_{\mathbb{R}} \frac{1}{\cosh(\theta - \theta')} L(\theta') d\theta'\right).$$

The kernel in the convolution defining $X(\theta)$ is $1/\cosh \theta = -i \frac{\partial}{\partial \theta} \log S_X(\theta)$, where

$$S_X(\theta) = \frac{1}{i} \frac{1 + ie^\theta}{1 - ie^\theta}.$$

Note that $S_X(0) = 1$, $S_X(\theta)S_X(-\theta) = 1$, and its nearest poles and zeros to the real axis are at $\pm i\pi/2$. This means that while the initial definition of $Y(\theta)$ holds in the strip $-\pi p < \text{Im } \theta < \pi p$, that of $X(\theta)$ holds in the wider strip $-\pi/2 < \text{Im } \theta < \pi/2$.

In [13] Zamolodchikov further showed that the X and Y functions just defined satisfy a number of functional relations, most succinctly expressed using an alternative parameter $a = 1 - 2p$. These are an X -system:

$$X\left(\theta + \frac{i\pi}{2}\right) X\left(\theta - \frac{i\pi}{2}\right) = 1 + X\left(\theta + \frac{ia\pi}{2}\right) X\left(\theta - \frac{ia\pi}{2}\right);$$

a Y -system:

$$Y\left(\theta + \frac{i\pi}{2}\right) Y\left(\theta - \frac{i\pi}{2}\right) = \left(1 + Y\left(\theta + \frac{ia\pi}{2}\right)\right) \left(1 + Y\left(\theta - \frac{ia\pi}{2}\right)\right);$$

and a couple of ‘ X - Y -systems’:

$$\begin{aligned} X\left(\theta + \frac{ia\pi}{2}\right) X\left(\theta - \frac{ia\pi}{2}\right) &= Y(\theta); \\ X\left(\theta + \frac{i\pi}{2}\right) X\left(\theta - \frac{i\pi}{2}\right) &= 1 + Y(\theta). \end{aligned}$$

Under duality, a maps to $-a$ and all of these relations map to themselves.

Unlike the more familiar Y -systems associated with relevant perturbations of many rational conformal field theories (see for example [12, 10]), these functional equations do not imply any straightforward periodicity properties for their solutions. As discussed in [13], this is associated with the subtleties of the UV behaviour of

the sinh-Gordon model. Here we just add two further remarks. First, at the self-dual point $p = 1/2$, the X -system reduces to $X\left(\theta + \frac{i\pi}{2}\right)X\left(\theta - \frac{i\pi}{2}\right) = 1 + X(\theta)^2$. After a trivial relabeling this is the recurrence relation associated with the simplest cluster algebra of infinite type, namely $A_1^{(1)}$, a (non-periodic) closed form solution to which was found in [14]. Second, in the small-coupling, $p \rightarrow 0$ limit we have $a = 1 - 2p \rightarrow 1$ and the two X - Y systems might appear to come into conflict. However this is not the case: for $X(\theta)$, the factor of $\exp\left(-\frac{r}{2\sin(\pi p)} \cosh(\theta)\right)$ in its initial definition comes to dominate in the $p \rightarrow 0$ limit, so that

$$X(\theta) \rightarrow \begin{cases} 0 & |\operatorname{Im} \theta| < \pi/2 \\ \infty & \pi/2 < |\operatorname{Im} \theta| < 3\pi/2 \end{cases}$$

and so on. This explains the apparent disagreement between the two X - Y -systems at $p = 0$: the left-hand sides of these equations cease to be well-defined in this limit. It is possible to get finer control of this limit, and get to an X - Y -system which continues to make sense when $p \rightarrow 0$, by defining, for $|\operatorname{Im}(\theta)| < \frac{\pi}{2}$,

$$\tilde{X}(\theta) = \exp\left(\frac{1}{2\pi} \int_{\mathbb{R}} \frac{1}{\cosh(\theta - \theta')} L(\theta') d\theta'\right)$$

so that

$$X(\theta) = e^{-\frac{r}{2\sin(\pi p)} \cosh(\theta)} \tilde{X}(\theta).$$

The X and X - Y systems become the following \tilde{X} and \tilde{X} - Y systems:

$$\begin{aligned} \tilde{X}\left(\theta + \frac{i\pi}{2}\right) \tilde{X}\left(\theta - \frac{i\pi}{2}\right) &= 1 + e^{-r \cosh \theta} \tilde{X}\left(\theta + \frac{i\pi}{2}\right) \tilde{X}\left(\theta - \frac{i\pi}{2}\right) \\ \tilde{X}\left(\theta + \frac{i\pi}{2}\right) \tilde{X}\left(\theta - \frac{i\pi}{2}\right) &= e^{r \cosh \theta} Y(\theta) \\ \tilde{X}\left(\theta + \frac{i\pi}{2}\right) \tilde{X}\left(\theta - \frac{i\pi}{2}\right) &= 1 + Y(\theta) \end{aligned}$$

For $p = 0$, $a = 1$ these equations become

$$\begin{aligned} \tilde{X}\left(\theta + \frac{i\pi}{2}\right) \tilde{X}\left(\theta - \frac{i\pi}{2}\right) &= 1 + e^{-r \cosh \theta} \tilde{X}\left(\theta + \frac{i\pi}{2}\right) \tilde{X}\left(\theta - \frac{i\pi}{2}\right) \\ \tilde{X}\left(\theta + \frac{i\pi}{2}\right) \tilde{X}\left(\theta - \frac{i\pi}{2}\right) &= e^{r \cosh \theta} Y(\theta) \\ \tilde{X}\left(\theta + \frac{i\pi}{2}\right) \tilde{X}\left(\theta - \frac{i\pi}{2}\right) &= 1 + Y(\theta) \end{aligned}$$

and are no longer inconsistent. Indeed, equating the right-hand sides of the second and third equations implies that, in this limit, $Y(\theta) = 1/(e^{r \cosh \theta} - 1)$, a result which will be found by other means in the next section. However we should add a caveat

that this is only consistently the limiting form of $Y(\theta)$ in the region $|\text{Im } \theta| < \pi/2$. For $\pi/2 < |\text{Im } \theta| < \pi$, our numerical results show that $Y(\theta)$ develops singularities along a zig-zag pattern of lines as $p \rightarrow 0$, as illustrated in Figs. 3 and 4 below.

3 A subtlety in the small- p limit

As $p \rightarrow 0$ the kernel $\phi(\theta)$ becomes increasingly concentrated near $\theta = 0$. Taking the limit, $\phi(\theta - \theta')$ can be replaced by $2\pi\delta(\theta - \theta')$ in the convolution term in the TBA equation, which becomes

$$\varepsilon(\theta) = r \cosh \theta - \int_{\mathbb{R}} \delta(\theta - \theta') L(\theta') d\theta' = r \cosh \theta - L(\theta).$$

Exponentiating and solving recovers the formula for $Y(\theta)$ given at the end of the previous section:

$$Y(\theta) = e^{-\varepsilon(\theta)} = 1/(e^{r \cosh \theta} - 1).$$

Substituting into the formula for $c(r)$,

$$c(r) = -\frac{3}{\pi^2} \int_{\mathbb{R}} r \cosh \theta \log(1 - e^{-r \cosh \theta}) d\theta.$$

Apart from some signs, this is very similar to the integral formula for $c_0^{(\text{Ising})}(r)$ reported in the introduction. In fact, and perhaps unsurprisingly, it precisely matches $c_0^{(\text{boson})}(r)$, the effective central charge for a single free boson [9]. Just as for the Ising field theory, an alternative formula exists which makes its analytic structure clear:

$$\begin{aligned} c_0^{(\text{boson})}(r) &= 1 - \frac{3r}{\pi} + \frac{3r^2}{2\pi^2} \left(\log \frac{1}{r} + \frac{1}{2} + \ln 4\pi - \gamma_E \right) \\ &\quad - \frac{6}{\pi} \sum_{k=1}^{\infty} \left(\sqrt{r^2 + (2k\pi)^2} - 2k\pi - \frac{r^2}{4k\pi} \right). \end{aligned}$$

This time, the predicted branch points are at even integer multiples of $i\pi$, in contrast to the odd integer multiples seen for the Ising field theory. But more crucially, the *signs* of the square root terms are reversed. When continuing $c_0^{(\text{Ising})}(r)$ around branch points from the ground state, the resulting flips in signs of square roots led to an *increase* in $E(m, R)$, and excited state energies which were higher than that of the ground state. But with the square roots in the formula for $c_0^{(\text{boson})}(r)$ starting with the opposite signs, any flips will *decrease* the corresponding $E(m, R)$, leading to ‘states’ with lower energy than the ground state. Since this cannot be correct, the whole analytic continuation programme might be questioned. Fortunately, it can be argued that the case of the free boson is genuinely exceptional.

Consider first a (rather standard) toy example: the quantum mechanical simple harmonic oscillator, which can be thought of as a free boson in a universe with just one point. The eigenvalue problem is

$$\left(-\frac{d^2}{dx^2} + v^2 x^2\right) \psi(x) \equiv \mathcal{H}_v \psi(x) = E \psi(x)$$

with v a real parameter, and the energy levels, found by imposing $\psi \in L^2(\mathbb{R})$, are

$$E_n = (2n + 1)v \quad n = 0, 1, 2, \dots$$

Now, in analogy with the continuations performed earlier, set $v = re^{i\phi}$, with r and ϕ real, and continue ϕ from 0 to π . Then v continues to $-v$ and all the energies change sign (and thus decrease), even though under the continuation $\mathcal{H}_v \rightarrow \mathcal{H}_{-v} = \mathcal{H}_v$, so the eigenvalue problem might appear to be unchanged. The resolution of this apparent paradox comes from realising that eigenvalue problems associated with differential operators are specified not only by the differential operator, but also by the boundary conditions that are imposed. For the simple harmonic oscillator, the continuation just described rotates the associated Stokes sectors by ninety degrees, which in turn moves the contour along which the wavefunction must be square integrable from \mathbb{R} to $i\mathbb{R}$ – and for this revised eigenvalue problem, the eigenvalues are indeed the negatives of their more usual values.

The same phenomenon occurs for two simple harmonic oscillators, coupled together, when the continuation is in their coupling [1]. This corresponds to a free boson in a universe with two points, with the ‘size’ of this universe relating to the strength of the coupling. Continuation on a closed path from the decoupling point and back can flip the boundary conditions and send energies to their negatives. However, this interference in the boundary conditions is only possible because the coupling between the oscillators is of the same quadratic order at infinity as the potential for each single oscillator. For more severely confining potentials such as the hyperbolic cosine found in the sinh-Gordon model, this is not the case and a continuation in system size would not be expected to flip boundary conditions from their starting configurations. In the absence of a detailed theory of the Stokes sectors for the relevant functions of many variables, the reasoning just given is far from being rigorous. However our numerical work has confirmed that for the sinh-Gordon model, continuation in r at fixed but nonzero p , no matter how small p is taken to be, always leads to states of higher, not lower, energies. This implies that the process of analytic continuation in r does not commute with the taking of the $p \rightarrow 0$ limit, and so the surprising (and unfortunate) continuation of the ground state energy when p is strictly zero should not deter us from its study for $p > 0$.

As a last remark we note that the at first sight surprising continuation properties of the free boson ground state energy have an analogue in the behaviour of $T\bar{T}$ -deformed conformal field theories with $c_{\text{eff}} > 0$ [4]. In that context the branch point occurs for physical values of R and is interpreted as a Hagedorn singularity. It would be interesting to investigate whether the considerations just given might be

relevant for understanding the otherwise mysterious level that is found on continuation around this point.

4 Numerical results

In this section, we outline some of the results we have obtained from numerical work on the sinh-Gordon TBA, focusing on small but non-zero values of p . The picture we find is not yet complete, and we hope to be able to give a more comprehensive description elsewhere.

The procedure we followed is as described in the introduction. First we solved the ground state TBA to find the effective central charge $c_0(r)$ in the complex r plane². A typical plot, for $p = 0.04$, is shown in Fig. 1 (a). For sufficiently negative values of $\text{Re}(r)$, iteration of the TBA equation failed to converge no matter how strongly it was damped, and these regions are left blank on the figure³. Along the edge of this region lies a sequence of branch points, labeled on the figure with the letters $A \dots D$ and $A' \dots D'$, all of which turn out to be of square root type. As $p \rightarrow 0$, the locations of these branch points tend to even multiples of $2\pi i$: those at A and A' to $2\pi i$, those at B and B' to $4\pi i$, and so on. As the TBA system is continued around these branch points, pairs of points in the complex θ plane at which $e^{-\varepsilon(\theta)} = -1$ cross the contour of integration, converting the equation into an excited-state equation in the manner reviewed in the introduction. Continuation back to the real axis results in excited states which in the infrared, that is for large real values of r , contain two particles with equal and opposite momenta, and Bethe quantum numbers ± 1 for A and A' , ± 2 for B and B' , and so on. It is worth noting that continuation about paired branch points such as A and A' leads to the *same* excited state; given that all branch points are square roots, this means that continuation along a loop encircling both but no others is monodromy free.

Once the relevant excited state TBA equations have been identified, plots can be made of the scaling functions implied by these equations. One such plot is shown in Fig. 1 (b), again for $p = 0.04$, and two more are in Figs. 2 (a) and (b). The branch points on these plots which connect back to the ‘parent’ ground state energy level are indicated with the corresponding letters; there are also further branch points, which connect not with the ground state, but rather with more highly-excited levels, with more than two particles in the infrared. Continuing around these points, we have been able to connect with states containing 4 and then 6 particles, and there seem to be no obstacles to going further. Given that the $\theta \rightarrow -\theta$ symmetry of the ground-state TBA is preserved under continuation, the states we find are always

² We should note that, as done in previous work [6, 7], even for the ground state it was necessary to deform the contour of integration in the convolution term to lie a little below the real axis at $+\infty$, and above it at $-\infty$, in order to extend to values of r with argument larger than $\pi/2$.

³ In the $p \rightarrow 0$ limit this convergence failure can be understood analytically, as will be explained in the next section.

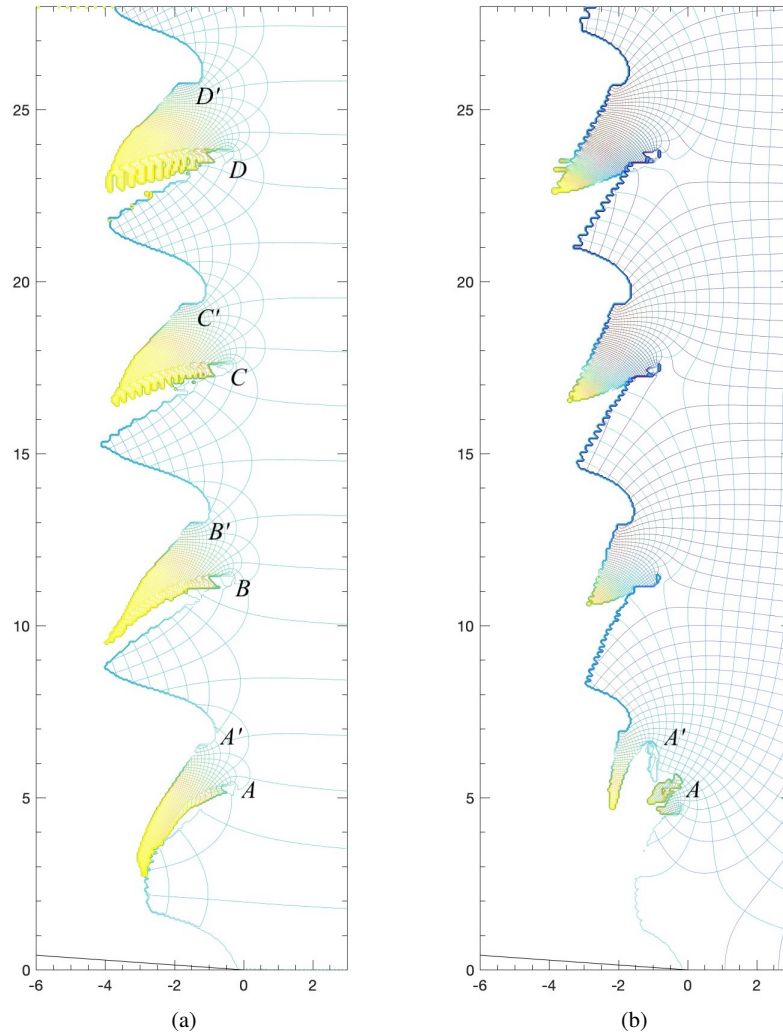


Fig. 1 Contour plots of the real and imaginary parts of the $p = 0.04$ sinh-Gordon effective central charge $c_0(r)$ (a), and of the scaling function $c(r)$ for the lowest two-particle excited state (b). Horizontal and vertical axes correspond to the real and imaginary parts of r , while the letters $A \dots D$ and $A' \dots D'$ label selected square-root branch points, described further in the main text.

symmetrical with respect to a negation of all momenta, but we did not observe any other restrictions on the set of states that can be reached.

To perform these continuations, it is important to keep track of the places where singularities (in the sense given in the introduction) of the pseudoenergies approach the real axis. For this purpose we used the X -system to continue $X(\theta)$ beyond the strip $-\pi/2 < \text{Im } \theta < \pi/2$ on which it is initially defined, and then the X - Y system

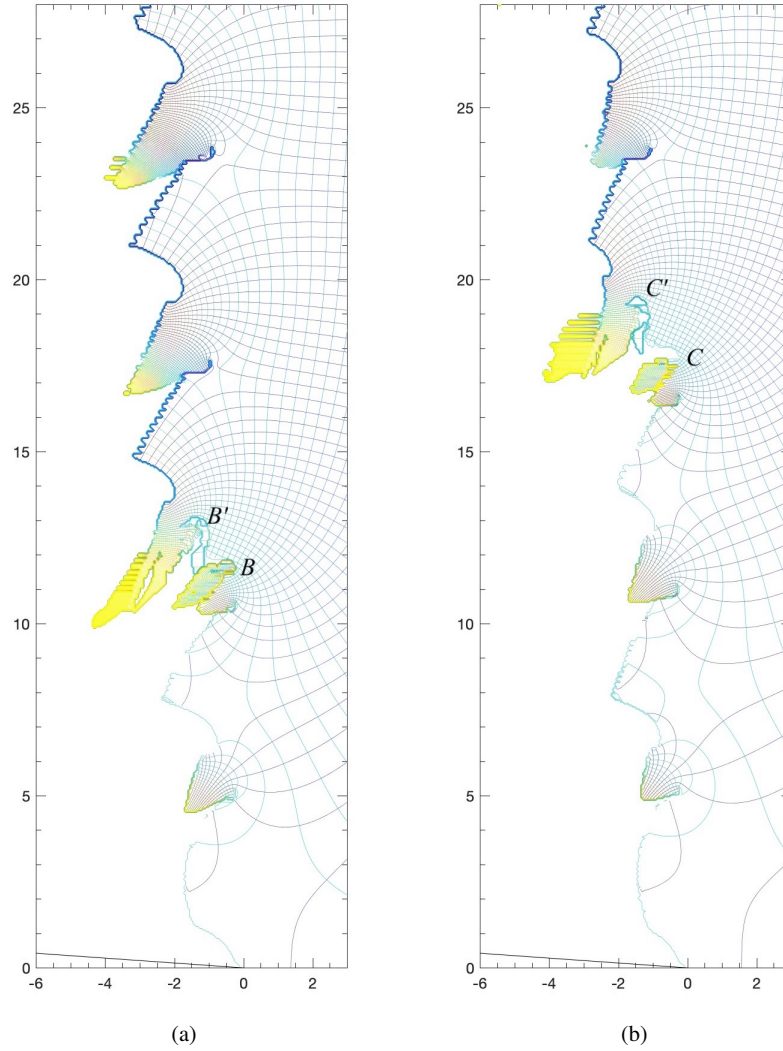


Fig. 2 Contour plots of the real and imaginary parts of the scaling function $c(r)$ for the second- and third-lowest symmetrical two-particle excited states of the $p = 0.04$ sinh-Gordon model, with Bethe quantum numbers $N = \pm 2$ (a) and $N = \pm 3$ (b).

to reconstruct $Y(\theta)$. For small values of p , high precision is needed in order to eliminate numerical artifacts; we used the Advanpix toolbox in Matlab [8].

The plots shown in Figs. 3 and 4, all computed for $r = 1$, illustrate the surprising behaviour of the ground state pseudoenergy as the small- p limit is taken at real values of r . They show contours of $Z(\theta)/(1 + Z(\theta))$, where $Z(\theta) = |1 + Y(\theta)|$. This function lies between zero and one and its zeros are the ‘singularities’ of the pseu-

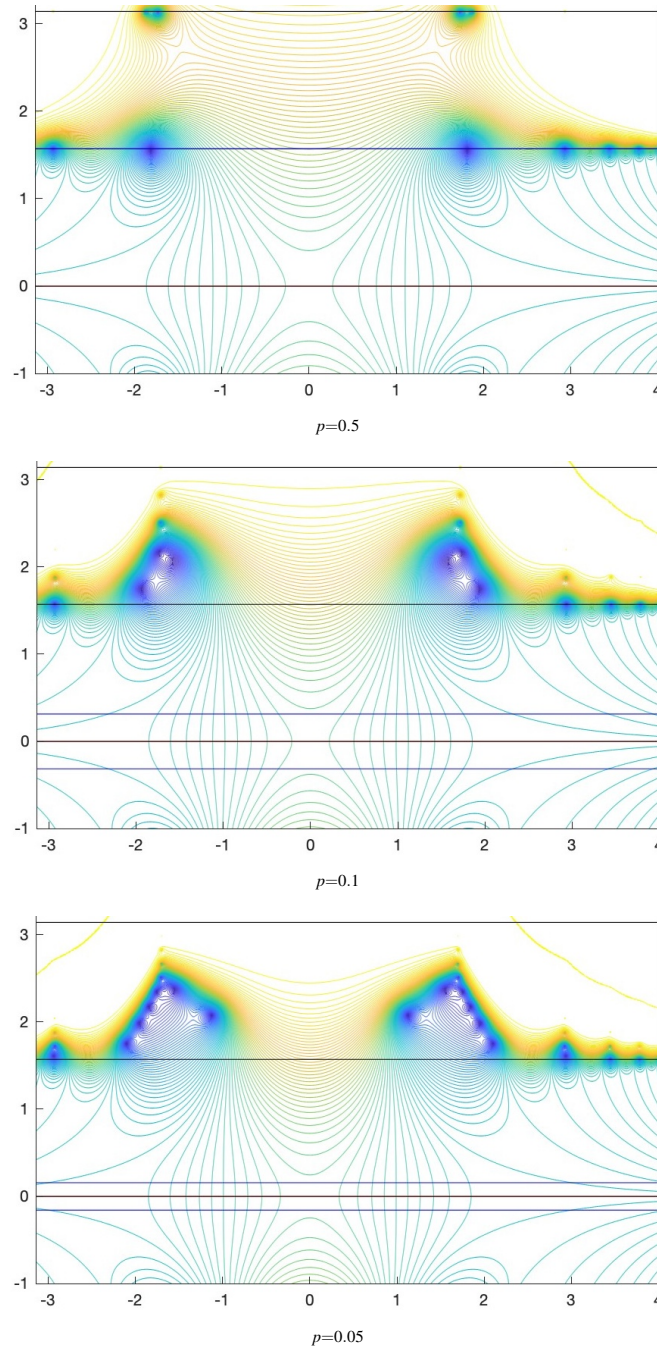


Fig. 3 Contour plots of $Z(\theta)/(1+Z(\theta))$ in the complex θ plane, where $Z(\theta) = |1+Y(\theta)|$, at various values of p , with $r = 1$. The horizontal lines lie at $\text{Im } \theta = -p\pi, 0, p\pi, \pi/2$ and π .

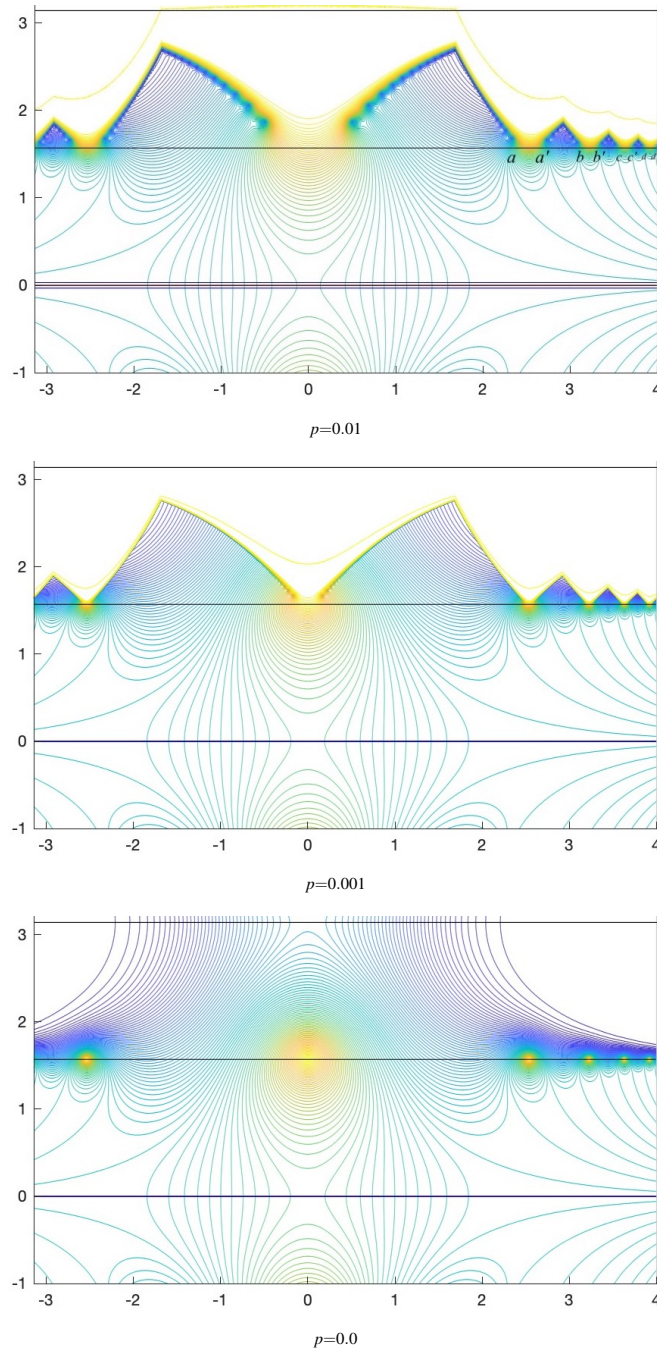


Fig. 4 Contour plots of $Z(\theta)/(1+Z(\theta))$ for further values of p , again with $r = 1$. For the final plot, $Y(\theta)$ is the function $1/(e^{r \cosh \theta} - 1)$ found in the formal $p \rightarrow 0$ limit, as discussed in the main text. The labels $a \dots d, a' \dots d'$ on the plot for $p = 0.01$ indicate zeros of $Z(\theta)$ which cross the real axis under continuation around the branch points $A \dots D, A' \dots D'$, respectively.

doenergy, that is the points at which $Y(\theta) = -1$. In a central strip $-\pi/2 < \text{Im}(\theta) < \pi/2$, we found that as $p \rightarrow 0$, the pseudoenergy tends smoothly to the $p = 0$ solution, shown in the final plot of Fig. 4, and $Z(\theta)$ is free of zeros. However, further from the real θ axis the situation becomes more complicated: zeros accumulate along a set of curves in the strip $\pi/2 < \text{Im}(\theta) < \pi$, resulting in a sequence of inverted Y-like structures in the upper half plane which spread out from a central pair of ‘cat ears’, while their mirror images are formed in the lower half plane. Though not visible on the plots, this pattern repeats itself at larger values of $|\text{Im}(\theta)|$.

During continuation around one of the ground state branch points shown in Fig. 1 (a), the pattern of zeros distorts, and a zero from the tip of one of the structures in the upper half plane crosses the integration contour into the lower half plane, while its negative makes the opposite journey. Together, they become the pair of ‘activated’ singularities at θ_0 and $-\theta_0$ in the excited-state TBA equation. The relevant singularities are indicated on the $p = 0.01$ plot of Fig. 4, and their pairing matches the pairing of ground state branch points seen in Fig. 1 (a): under continuation around branch point A , the singularity at a crosses to the lower half plane, while under continuation about A' , it is its neighbour at a' which crosses, and likewise for b and b' , c and c' , and d and d' . A similar picture is found for continuation of the excited state TBA equations.

5 TBA iteration in the small- p limit

One feature of the scaling function plots shown in the last section was the presence of regions of the complex r plane where iteration of the TBA equation failed to converge. In the small- p limit their boundary acquires a characteristic, somewhat sinusoidal, shape, which can be understood analytically.

We begin by writing the TBA equation as $\varepsilon = F[\varepsilon]$ where

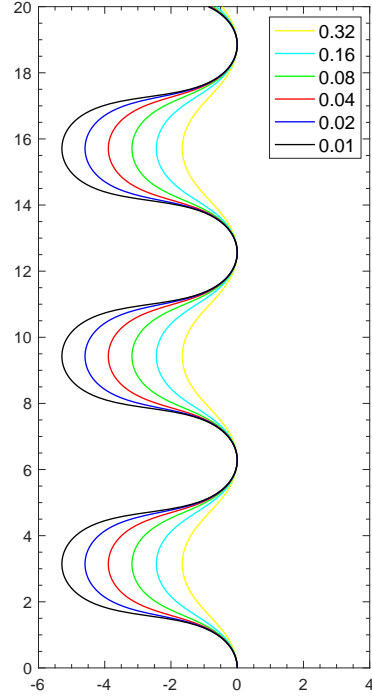
$$F[\varepsilon] = r \cosh \theta - \frac{1}{2\pi} \int_{\mathbb{R}} \phi(\theta - \theta') \log(1 + e^{-\varepsilon(\theta')}) d\theta'.$$

This can be solved numerically by iteration: $\varepsilon_{n+1} = F[\varepsilon_n]$. To help convergence it is useful to introduce a damping factor λ with $0 < \lambda \leq 1$ and instead iterate $\varepsilon_{n+1} = G_\lambda[\varepsilon_n]$ with $G_\lambda[\varepsilon] = (1 - \lambda)\varepsilon + \lambda F[\varepsilon]$. However even this does not always converge. In the limit $p \rightarrow 0$, we have $F[\varepsilon] = r \cosh \theta - \log(1 + e^{-\varepsilon(\theta)})$, the iterations at different values of θ decouple, and the lack of convergence can be understood as follows. Setting $r \cosh \theta = \hat{r}$, the fixed point ε_∞ for both the F and G iterations is the $p = 0$ TBA solution found earlier, satisfying $e^{\varepsilon_\infty} = e^{\hat{r}} - 1$. For this to be stable for $\varepsilon_{n+1} = G_\lambda[\varepsilon_n]$ we need $|G'_\lambda(\varepsilon_\infty)| < 1$, that is

$$|1 - \lambda + \lambda e^{-\hat{r}}| < 1,$$

or, with $\hat{r} = x + iy$,

Fig. 5 Convergence regions for the $p = 0$ TBA equation in the complex $r = x + iy$ plane, for various values of the damping factor λ . For the leftmost curve, $\lambda = 0.01$; for the rightmost, $\lambda = 0.32$. In all cases the convergence region is to the right of the curve shown.



$$|1 - \lambda + \lambda e^{-x-iy}|^2 = (1 - \lambda)^2 + 2\lambda(1 - \lambda)e^{-x} \cos(y) + \lambda^2 e^{-2x} < 1$$

which implies

$$\lambda e^{-2x} + 2(1 - \lambda)e^{-x} \cos(y) - 2 + \lambda < 0.$$

This is the region of the complex $x + iy$ plane to the right of the curve

$$x(y) = -\log \left(\frac{-(1 - \lambda) \cos(y) + \sqrt{(1 - \lambda)^2 \cos^2(y) + (2 - \lambda)\lambda}}{\lambda} \right).$$

The point $\theta = 0$, for which $\hat{r} = r$, always lies on the integration contour and so for convergence r must certainly lie in this region, which is shown for various values of λ in Fig. 5. The smaller the value of λ , the stronger the damping, and the larger the convergence region becomes. However, for $\cos(y) \neq 0$ and $\lambda \rightarrow 0$ we have

$$x(y) = -\log \left(\frac{(1 - \lambda) |\cos(y)|}{\lambda} \left(\sqrt{1 + \frac{(2 - \lambda)\lambda}{(1 - \lambda)^2 \cos^2(y)}} - \sigma \right) \right)$$

$$\sim \begin{cases} \log(\cos(y)) & \sigma = +1 \\ \log(\lambda/2) - \log |\cos(y)| & \sigma = -1 \end{cases}$$

where $\sigma = \text{sgn}(\cos(y))$. The fact that the limiting curve for $\sigma = +1$ is independent of λ means that in the $p \rightarrow 0$ limit there are ‘forbidden zones’ lying in the strips $|\text{Im}(r) - 2n\pi| < \pi/2$, $n \in \mathbb{Z}$, where the iterative algorithm does not converge no matter how strong the damping. This picture is consistent with our numerical results at small but nonzero values of p .

6 Conclusions

In this article we have shown that the analytic continuation of energy levels in the finite volume sinh-Gordon model simplifies significantly in the $p \rightarrow 0$ limit. However, much work remains to be done before we can claim to have a complete picture. In particular, it turns out that the branch points labeled in Fig. 1 (a) are not the only ones which are accessible from the ground state: there are others, hidden in the region where the numerical methods we have presented so far do not converge. Some of these can be glimpsed by allowing the convergence factor λ to become complex⁴, though we suspect that their detailed study will require a more sophisticated approach, possibly along the lines of that used in [3]. Our preliminary results indicate that these extra branch points lie on curves in the complex r plane terminating on the ground state branch points that were already discussed, condensing in the $p \rightarrow 0$ limit much as did the zeros of $Z(\theta)$ for the pseudoenergy. If so, this condensation should be relevant to a deeper understanding of the subtleties that were described in section 3, and shed light on the mechanism by which continuation to states of higher energy for nonzero values of p is flipped to a continuation to a shadow sector with lower energies when p is exactly equal to zero.

Acknowledgements We would like to thank David Meier for collaboration on early stages of this project, and Carl Bender, Lorenz Hilfiker, Didina Serban, István Szécsényi, Roberto Tateo and Pavel Tumarkin for helpful discussions and suggestions. PED thanks the MATRIX research institute, Australia, for hospitality, supported by a Simons Travel Grant. The work was also supported in part by a grant from the UK STFC, number ST/X000591.

References

1. Bender, C.M., Felski, A., Hassanpour, N., Klevansky, S.P., Beygi, A.: Analytic structure of eigenvalues of coupled quantum systems. *Phys. Scripta* **92**(1), 015,201 (2017). doi:10.1088/0031-8949/92/1/015201
2. Bender, C.M., Wu, T.T.: Anharmonic oscillator. *Phys. Rev.* **184**, 1231–1260 (1969). doi:10.1103/PhysRev.184.1231

⁴ In the calculations of the last section, λ was assumed, as is standard, to be real. If λ becomes complex the curves plotted in Fig. 5 shift, and in some cases, even for nonzero values of p , the iterations then converge in previously inaccessible regions. It was this which allowed us to detect the additional branch points.

3. Camilo, G., Fleury, T., Lencsés, M., Negro, S., Zamolodchikov, A.B.: On factorizable S-matrices, generalized T \bar{T} , and the Hagedorn transition. *JHEP* **10**, 062 (2021). doi:10.1007/JHEP10(2021)062
4. Cavaglià, A., Negro, S., Szécsényi, I.M., Tateo, R.: $T\bar{T}$ -deformed 2D Quantum Field Theories. *JHEP* **10**, 112 (2016). doi:10.1007/JHEP10(2016)112
5. Dorey, P., Hilfiker, L., Szécsényi, I.: Unpublished
6. Dorey, P., Tateo, R.: Excited states by analytic continuation of TBA equations. *Nuclear Physics B* **482**(3), 639–659 (1996)
7. Dorey, P., Tateo, R.: Excited states in some simple perturbed conformal field theories. *Nuclear Physics B* **515**(3), 575–623 (1998)
8. Holodoborodko, P.: Multiprecision Computing Toolbox for MATLAB 4.8.5.14569. Advanpix LLC., Yokohama, Japan (2021)
9. Klassen, T.R., Melzer, E.: The Thermodynamics of purely elastic scattering theories and conformal perturbation theory. *Nucl. Phys. B* **350**, 635–689 (1991). doi:10.1016/0550-3213(91)90159-U
10. Ravanini, F., Tateo, R., Valleriani, A.: Dynkin TBAs. *Int. J. Mod. Phys. A* **8**, 1707–1728 (1993). doi:10.1142/S0217751X93000709
11. Zamolodchikov, A.I. B.: Thermodynamic Bethe Ansatz in relativistic models: Scaling 3-state Potts and Lee-Yang models. *Nuclear Physics B* **342**(3), 695–720 (1990)
12. Zamolodchikov, A.I. B.: On the thermodynamic Bethe ansatz equations for reflectionless ADE scattering theories. *Phys. Lett. B* **253**, 391–394 (1991). doi:10.1016/0370-2693(91)91737-G
13. Zamolodchikov, A.I. B.: On the Thermodynamic Bethe Ansatz equation in sinh-Gordon model. *Journal of Physics A: Mathematical and General* **39**(41), 12,863 (2006)
14. Zelevinsky, A.: Semicanonical basis generators of the cluster algebra of type $a_1^{(1)}$. arXiv preprint math/0606775 (2006)